The 2009 IEEE/RSJ International Conference on
Intelligent Robots and Systems
October 11-15, 2009 St. Louis, USA

An Experimental Study and Modeling of Loading and Unloading of Nonlinear Viscoelastic Contacts

Chia-Hung Dylan Tsai and Imin Kao
Department of Mechanical Engineering
SUNY at Stony Brook, Stony Brook, USA

Kayo Yoshimoto, Mitsuru Higashimori
and Makoto Kaneko
Osaka University, Osaka, Japan

Abstract— **The latency model is an analytical model for describing the behavior of nonlinear viscoelastic contact interface in robotic grasping and manipulation. The latency model is based on experimental observation of viscoelastic materials which exhibit the behavior of both elastic and temporal responses when subject to external force or displacement. It is postulated that such materials display latency in response of external influence by the rearrangement of molecules, holes, and structures in order to achieve an equilibrium state corresponding to the instantaneous loading. As a result, we propose that there are temporal *latent activities* in progress before the material reaches the equilibrium state. In the previous study [21], the latent activity of strain re-distribution with a prescribed constant displacement was presented using both theoretical modeling and experimental results. In this paper, we build upon this latency model to study the behavior of viscoelastic materials under different loading rates with experimental results. The latency model is employed to explain the behavior of responses of hard and soft viscoelastic materials typically found in robotic contact and grasping.**

I. INTRODUCTION

Viscoelasticity has been broadly studied from many different perspectives; for example, the latency model [21], Fung's separation model [4], Maxwell model [13] and many other well-known models discussed in [6], [7], [3]. Creep and relaxation are two major phenomena of viscoelasticity when it comes to the tasks of robotic grasping and manipulation. There are quite a few studies in this area: Tiezzi and Kao applied Fung's model to soft contact [19] modeling; Sakamoto *et al.* designed a robotic hand based on the Maxwell model to handle viscoelastic objects [15], as well as many other studies of viscoelastic grasping and/or soft contact behaviors presented in [22], [21], [14], [8], [24], [23], [9], [10], [16], [1], [11], [12], [17], [2].

This paper builds upon the study of the latency model proposed in [21] to investigate the behaviors of grasping response observed in viscoelastic materials. The concept of "latency" refers to the latent activities in progress, while the state of viscoelastic material remains the same macroscopically (*e.g.* displacement or force remains the same after loading or unloading). In [21], the latent activity of strain redistribution was studied based on experimental results when the displacement is held constant in a grasping task.

In this paper, the strain hardening effect (or *stiffening effect*) is correlated with the latent activity postulated in the latency model, as observed from the experimental results. Furthermore, Gardel concluded that the stiffening effect is directly related to the concentration of cross-link structure [5], which can also correlate with the idea of uneven strain distribution in the latency model. The strain hardening effect in contact interface can complement the previously proposed latency model to explain the observed behavior under different loading/unloading rates presented with the experimental studies in this paper.

II. THE LATENCY MODEL FOR VISCOELASTIC CONTACT INTERFACE

The latency model is an analytical model for describing the nonlinear contact behavior of viscoelastic materials based on experimental observation. In the latency model, we postulate that the strain distribution within the viscoelastic material is a function of time. When a viscoelastic material is subject to external displacement, the unevenly distributed strain, from the immediate contact interface inward to core of the material, will result in an uneven stress distribution; consequently, a change of contact force on the contact surface will happen [21]. Re-arrangement and re-distribution of the transient state will ensue until an equilibrium state is achieved. When the displacement of the deformed object is held constant, the force will decrease exponentially as a result of the re-arrangement. This is commonly known as the *relaxation* response. Likewise, when the external force deforming the subject is held constant, the rearrangement will occur with a tendency to reach towards the equilibrium, resulting in the exponential change of displacement. This is known as the *creep* response. In [21], the latent activity of strain distribution when subject to a constant displacement was investigated.

Tsai and Kao applied the modified Fung's model to formulate the latency model to study the strain rate when a viscoelastic contact is subject to a constant displacement after the loading is completed, as follows [21]

$$\dot{\varepsilon}_c = m\varepsilon_c + l = -\nu_1(\varepsilon_c + \varepsilon_0) = -\nu_1(\varepsilon_c + \frac{N_0 c_0}{\alpha_c}) \quad (1)$$

or

$$\dot{\varepsilon}_c = -\nu_1(\varepsilon_c + \frac{N_0(1-c_1)}{\alpha_c}) \quad (2)$$

where $m = -\nu_1$, $l = -(N_0 c_0 \nu_1)/\alpha_c$, $\dot{\varepsilon}_c$ and ε_c are the strain rate and strain of material on the contact interface, ε_o is the equilibrium strain for a given displacement, N_0 is the initial elastic response (force) due to the constant displacement after

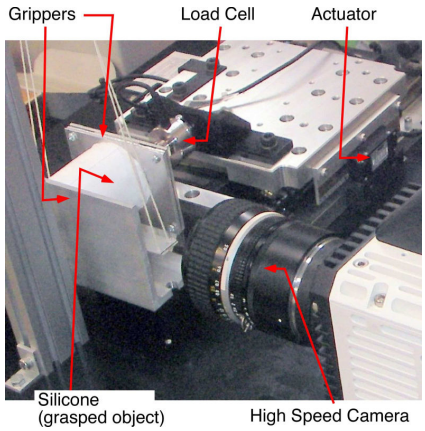

Fig. 1. Experimental setup for the compressive loading and unloading tests, showing the parallel-jaw gripper, camera, and ancillary devices

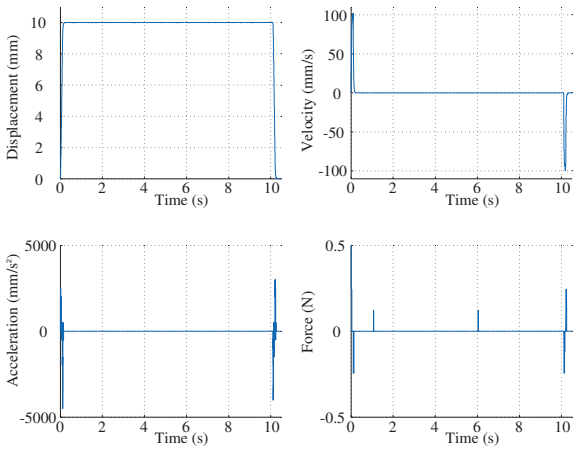

Fig. 2. The profiles of motion of the gripper from which the acceleration is determined to judge the inertial effect of gripper in experiments. The bottom right plot shows the measured inertial force from the load cell.

loading, and c_0, v_1, α_c are constant coefficients pertaining to the materials and their properties. The coefficients are defined in the following equation [21], [18], [19], [20]

$$F(t) = N_0(c_0 + c_1 e^{-v_1 t}) \quad \text{with} \quad c_0 + c_1 = 1 \tag{3}$$

In this paper, we study the force response based on different loading/unloading rates. The specific stiffness, k_s, in the paper is defined as

$$k_s = \frac{\partial \sigma}{\partial \varepsilon} \tag{4}$$

where σ and ε are the stress and strain, respectively.

III. EXPERIMENT AND ANALYSIS

In this section, we present the experimental setup first, followed by the experimental results and analysis.

A. Experimental setup

Figure 1 illustrates the experimental setup of a robotic parallel-jaw gripper and high-speed video camera. A grasped object is shown between the two gripper surfaces. The force of grasping is measured by the load cell mounted on the gripper that has an accuracy of $0.25N$. The accuracy of displacement of the system is $1\mu m$.

The mass of the gripper mounted on the load cell is $14\,g$, which moves with an acceleration up to $5000\,mm/s^2$ in all the experiments performed in this paper. The grasped object has much smaller movement and thus its inertial effect is neglected. As a result, we can estimate the maximum amount of inertial force to be about $0.07N$ (during the ramp-up and ramp-down periods). This is much smaller than the accuracy level of the force sensor. The actual profile of motion, measured inertial force, and the estimated inertial force are shown in Figure 2. By comparing the data of force with the gripper moving at the highest loading rate versus that of stationary gripper, the same conclusion is also reached. That is, the inertial effect due to the acceleration at the loading or unloading in this experimental setup can indeed be neglected.

Two different silicone solids with "hard" and "soft" texture are fabricated for the experimental study, as shown in

Fig. 3. The left and right cylindrical specimens are "hard" and "soft" silicone, respectively. The dimensions of both specimens are $25\,mm$ in radius and $30\,mm$ in height.

Figure 3. Both cylindrical silicones are 25mm in radius and 30mm in height with the compositions listed in Table I.

Figure 4 shows a schematic of the experimental setup in Figure 1 with the grasped silicone solid and the fiducial marks, parallel-jaw gripper, and the camera.

The procedures of the various experiments conducted under different loading rates are enumerated in the following.

1) The gripper is moved to barely touch the surface of the silicone solid. The silicone solid is supported freely by strings so that it will not fall due to gravity, but with least amount of interference to grasping.
2) The loading process will begin based on a loading rate determined *a priori* by the amount of prescribed displacement and the duration of holding (for relaxation). Several loading rates are employed as follows: 20, 40, 60, 80, and $100\,mm/sec$.
3) After the loading-and-hold procedure, the gripper unloads to break contacts, as shown in Figures 5 and 6.

The measurements of force and displacement, as well as the video camera capture are stored for further analysis.

TABLE I

COMPOSITION OF THE SILICONE USED IN THE EXPERIMENTS

	silicone powder	thinner
hard silicone	90%	10%
soft silicone	50%	50%

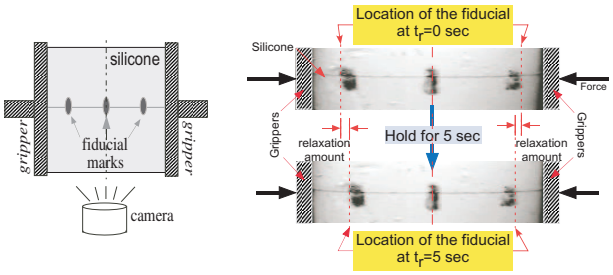

Fig. 4. *Left*: The schematic of the grippers, camera and silicone object. *Right*: Still photos in grasping from the experiment showing the relation and movement of the fiducial marks on the surface of the silicone solid, with the displacement being held at constant for 5 seconds.

B. Experimental results and analysis

1) Evidence of latency in relaxation: Figure 4 shows two still photo frames captured during holding after the loading phase is completed, to demonstrate the effect of relaxation. The first frame was captured when the loading process ended, followed by the beginning of the holding process at $t_r = 0\,sec$. The second fame was captured $5\,sec$ after holding at $t_r = 5\,sec$. We can clearly observe in Figure 4 the change of positions of the fiducial marks during the elapsed time. Hence, we use this as an evidence of ongoing rearranging activities, so called "latent activities", during holding (constant displacement of compression). The position change follows an exponential function of time [21].

2) Loading phase under different loading rates: Figures 5 and 6 show, for soft and hard silicone solids, respectively, the force measured under different loading rates, subject to a prescribed displacement controlled sequence.

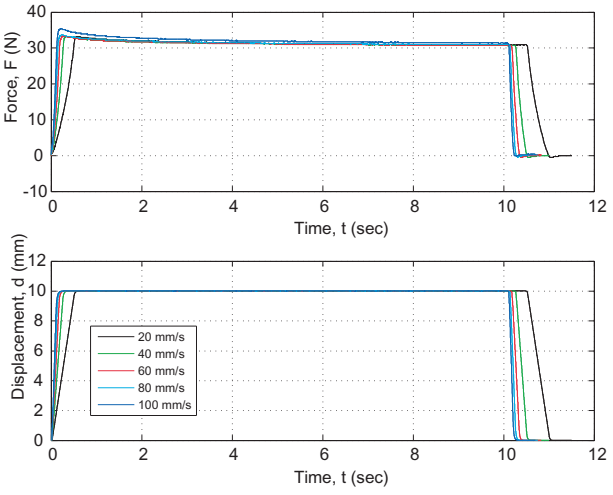

Fig. 5. The loading-holding-unloading process on soft silicone.

The viscoelastic materials share similar properties with elastic materials. First of all, the specific stiffness (defined by $\partial\sigma/\partial\varepsilon$ in equation 4) is different between soft and hard silicone solids in Figures 5 and 6. With the same amount of compression, the hard silicone shows higher specific stiffness and results in higher compression force.

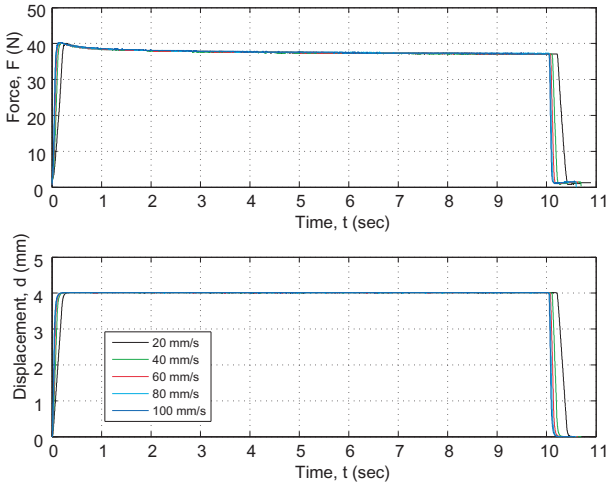

Fig. 6. The loading-holding-unloading process on hard silicone.

Different properties are observed in Figures 7 and 8 which show the zoom-in views of forces, focusing on the end of loading phase in Figures 5 and 6, respectively. We found that the maximum compressive forces of soft silicone due to different loading rates are different, with higher loading rate producing higher maximum compressive force, as shown in Figure 7. On the other hand, the maximum compressive force of the hard silicone due to different loading rates are nearly the same, as shown in Figure 8.

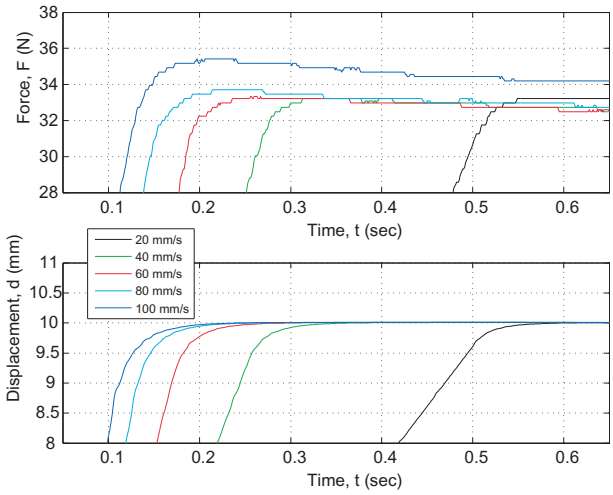

Fig. 7. The zoom-in views of the force and displacement curves towards the end of the loading phase in Figure 5 for the soft silicone.

3) Holding phase under different loading rates: Next, let us focus on the end of holding phase shown in Figures 9 and 10. It appears that the asymptotic values of relaxation curves under different loading rates are the same for both hard and soft silicone, although the responses start with different initial values as shown in Figures 7 and 8. This suggests that the equilibrium state (i.e., the asymptotic value of relaxation) is related to the held displacement, but not dependent upon the loading rates. In other words, the asymptotic value is a path-independent property for viscoelastic

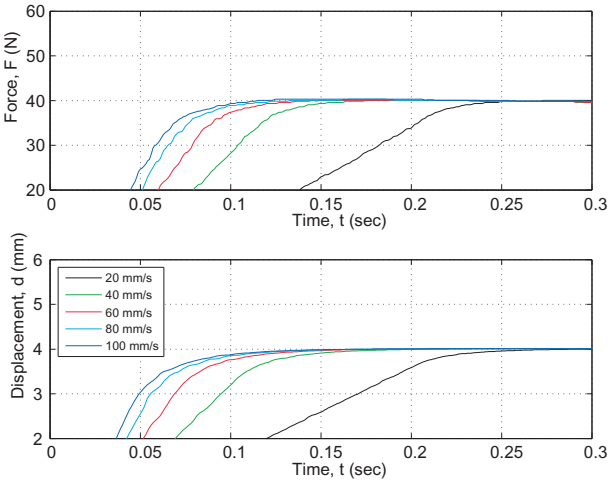

Fig. 8. The zoom-in views of the force and displacement curves towards the end of the loading phase in Figure 6 for the hard silicone.

material with a constant displacement.

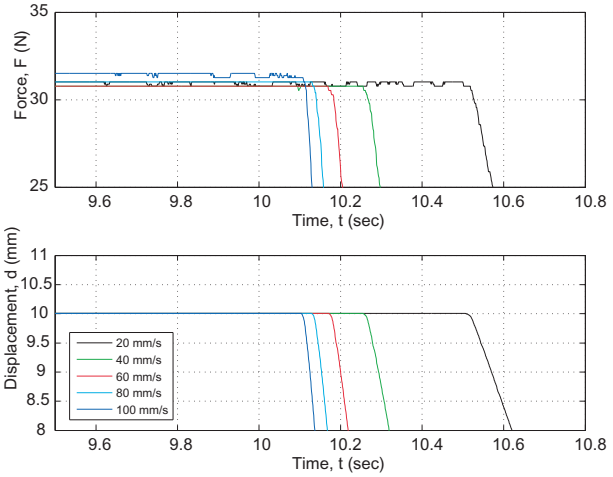

Fig. 9. The zoom-in views of the force and displacement curves towards the end of the holding phase for the soft silicone in Figure 5.

IV. DISCUSSIONS

A. Loading rates and the latency model

From the perspective of the latency model, the reaction force on a gripper is proportional to the stress on the contact surface. When the loading rate is high, the magnitude of strain on the contact surface will be high. The result of different maximum force in Figure 7 is due to the different loading process. When the loading rate is high, it does not allow the material enough time to re-distribute, and thus the build-up of force away from the equilibrium state is larger. The equilibrium state corresponds to the asymptotic state of the relaxation process. However, in the case of the hard silicone the maximum force of the higher loading rate is only slightly larger than that of the lower loading rate.

To apply the latency model to the experimental results, we first convert the measured force into stress on the contact

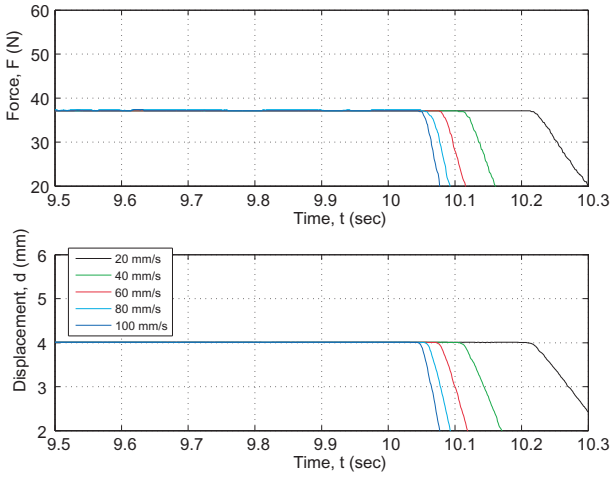

Fig. 10. The zoom-in views of the force and displacement curves towards the end of the holding phase for the hard silicone in Figure 6.

TABLE II

THE MATERIAL PROPERTY OF THE SPECIMEN

	ν_1 Equation (1)	$k_s(N/m^2)$ Specific Stiffness	ν Poisson Ratio
hard silicone	0.695	1.221×10^5	0.48
soft silicone	0.493	3.497×10^4	0.48

surface, $\sigma = F/A_n$. Next, the strain is obtained using equation (4) at the steady-state (asymptotic) values with $\varepsilon = k_s\sigma$. The following derivation renders the nominal contact area with different loading displacements. The variables are corresponding to Figure 11 where A is the original contact area, ΔA is the change of contact area due to the Poisson effect, ν is the Poisson ratio which is 0.48 from the specification of the silicone, and d, Δd, l, and Δl are geometric parameters. We have

$$A + \Delta A = \frac{\pi}{4}(d+\Delta d)^2 = \frac{\pi d^2}{4}(1-\frac{\nu \Delta l}{l})^2 \qquad (5)$$

The specific stiffness obtained from the asymptotic values at the end of loading is

$$k_s = \frac{\sigma_{asym}}{\varepsilon_{asym}} = \frac{F_{asym}/A_n}{\varepsilon_{asym}} \qquad (6)$$

where σ_{asym} and ε_{asym} are the asymptotic values of stress and strain on the contact surface, F_{asym} and A_n are the corresponding force measured by load cell and nominal contact area. The specific stiffness is a constant where the steady-state temporal response is established asymptotically. The properties of the silicone specimen are listed in Table II

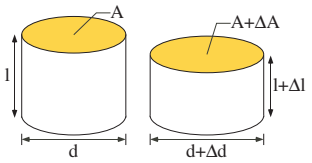

Fig. 11. Change of nominal contact area due to the Poisson effect

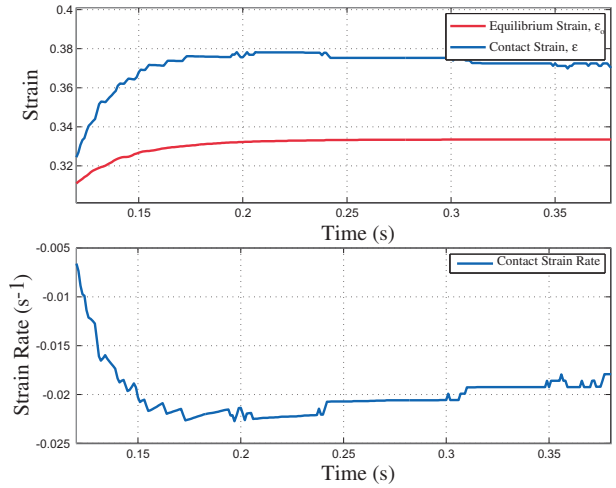

Fig. 12. This figure shows an example of the strain on the contact surface of soft silicone at the end of *loading phase*. The loading rate is $100mm/s$.

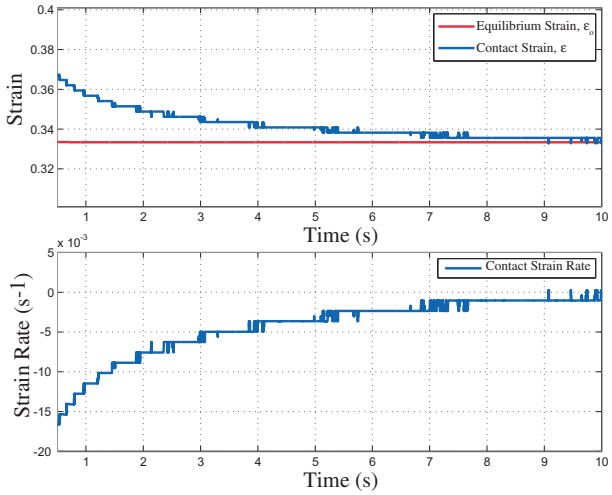

Fig. 13. This figure shows an example of the strain on the contact surface of soft silicone during the *relaxation phase*. The loading rate is $100mm/s$.

Following the steps above, we can obtain the strain at every moment during grasping by the following equation:

$$\varepsilon = \frac{\sigma}{k_s} = \frac{F/A_n}{k_s} \tag{7}$$

where σ is the stress on the contact surface, k_s is the specific stiffness of the material, F is the force measured by the load cell on the gripper, and A_n is the nominal contact area. Based on the conclusion of [22], the exponent of force relaxation curve will be consistent for the same material. Thus, we can obtain ν_1 by applying curve fitting to the relaxation curves in the form of equation (3). Consequently, we found $\nu_{1(soft)} = 0.493$ for the soft silicone and $\nu_{1(hard)} = 0.695$ for the hard silicone, listed in Table II.

The latency model shown in equation (1) still requires the equilibrium strain, ε_o. We note that the material will be uniformly distributed at the final equilibrium state. Therefore, the equilibrium strain is

$$\varepsilon_o = \frac{\Delta l}{l} \tag{8}$$

where ε_o is the strain at equilibrium state, Δl is the compression displacement, and l is the initial length of the material.

Now we can substitute the values from the experimental results into equation (1) and obtain the strain rate, $\dot{\varepsilon}_c$, during the operation. Figures 12 and 13 show the results of the analysis at the end of loading phase and during the relaxation, respectively. (For the convenience of reading, we plot the compression strain as positive in the figures which originally is negative.) Since the loading rate of the grippers is much faster than the strain rate inside the material, it results in larger strain on the contact surface than the equilibrium strain at the loading phase (the first plots in Figure 12). The second plot is the internal strain rate of material obtained from the latency model in equation (1).

This phenomenon is consistent with the latency model that utilizes the re-arrangement and re-distribution of structures and molecules in order to achieve a new equilibrium based on the external force or displacement.

B. Asymptotic value of relaxation and the latency model

The asymptotic value of relaxation curves is found to be the same, and depends on the material and the total external force. If the same external force is applied to a viscoelastic object, the equilibrium state will be the same when the time approaches infinity, regardless of the loading rate. This also suggests that the strain/stress distribution will be uniform for any isotropic material.

In Figure 13, the analysis of relaxation phase is shown. The first plot shows that the actual strain (blue curve) on the contact surface initially is greater than the equilibrium strain (red curve). However, the strain on the contact surface will eventually reach the equilibrium value. Thus, the results match with the prediction of the latency model very well.

The existence of the asymptotic value is predicted by the latency model in that the localized strained states will return to its equilibrium state when the disturbance is removed with the change of strain given in equation (1).

C. Strain stiffening/hardening and the latency model

Strain stiffening, a well-known phenomenon, delineates the increase of stiffness at the contact interface when an external force is applied. Instead of considering the stiffening effect being due to the change of the material property called *stiffness*, the latency model provides an alternative explanation of the effect in the sense of uneven strain distribution inside the viscoelastic material. Because the strain propagation inside viscoelastic material is slower than the loading rate applied by the external force, as presented in the preceding experimental results, an uneven strain distribution will be created. To this end, a higher loading rate will result in a more uneven strain distribution. A comparison of material movement between a high and a low loading rate is illustrated in Figure 14. We notice that at the end of loading, the strain on the contact surface (yellow shade area) will be higher at the high loading rate than low loading rate, resulting in the difference of reaction forces for the

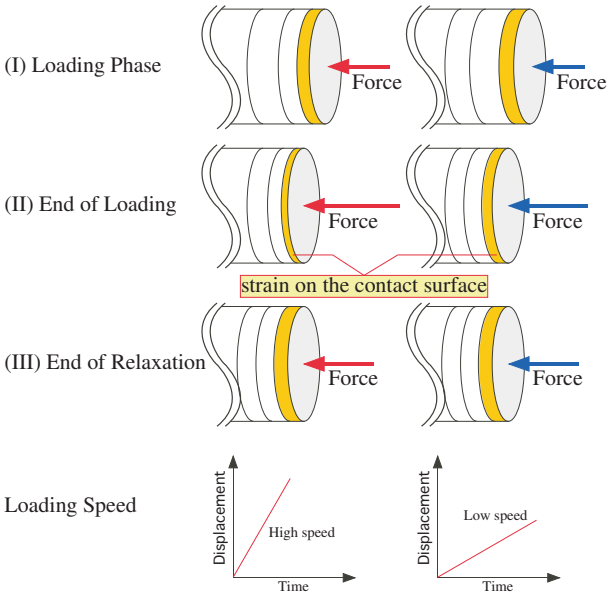

Fig. 14. This figure illustrates the idea of the latency model with different loading rates. The left and the right columns show the change of the strain on the contact surface with high and low loading rates, respectively. We observe in (I) and (II) that the strain distribution is not even during loading and at the end of loading. With the same displacement being held, the material tends to rearrange the strains when enough time is allowed, as shown in (III), and the strain distribution becomes more uniform.

same amount of displacement compression. This is known as the strain stiffening effect. When time is allowed for the uneven strains to propagate and reach a new equilibrium state, the asymptotic reaction force will then become the same again. This has been presented experimentally in this paper, as illustrated in (III) in Figure 14.

V. CONCLUSION

In this paper, we present the results of experimental studies and modeling of the latency model as applied to the loading and unloading of viscoelastic materials in contact. We found that the latency model is consistent with the well-known strain stiffening/hardening effect. From the perspective of the latency model, this effect can be explained by the uneven strain distribution inside the material. We also deduce from the experimental results that there is an asymptotic equilibrium state of the viscoelastic material when subject to external force or displacement. It depends on the property of the material and the external force or displacement applied, but not on the loading rate. The latency model can be applied to explain the experimental results of relaxation observed in a displacement-controlled grasping task.

VI. ACKNOWLEDGEMENT

This research has been supported by the NSF (National Science Foundation) Grants CMS0428403 and CMMI0800241, as well as a grant from JST H19/299-1 (Japan Science and Technology Agency).

REFERENCES

[1] F. Barbagli, A. Frisoli, K. Salisbury, and M. Bergamasco. Simulating human fingers: a soft finger proxy model and algorithm. In *Proc. IEEE Int. Symp. on Haptic Interface, HAPTICS'04*, 2004.

[2] L. Biagiotti, P. Tiezzi, C. Melchiorri, and G. Vassura. Modelling and identification of soft pads for robotic hands. In *Proc. IEEE Int. Conf. on Intelligent Robots and Systems, IROS*, Edmonton, Canada, 2005.

[3] W. Flugge. *Viscoelasticity*. Blaisdell Publishing Company, 1967.

[4] Y. C. Fung. *Biomechanics: Mechanical Properties of Living Tissues*. Springer-Verlag, 1993.

[5] M. L. Gardel, J. H. Shin, F. C. MacKintosh, L. Mahadevan, P. Matsudaira, and D. A. Weitz. Elastic behavior of cross-linked and bundeled actin networks. *Science*, 304:1301–1305, May 2004.

[6] T. G. Goktekin, A. W. Bargteil, and J. F. O'Brien. A method for animating viscoelastic fluid. In *Special Interest Group on Graphics and Interactive Techniques, SIGGRAPH*, 2004.

[7] A. Z. Golik and Y. F. Zabashta. a molecular model of creep and stress relaxation in crystalline polymers. *Mekhanika Polimerov*, pages 969–975, 1971.

[8] R. D. Howe, N. Popp, I. Kao, P. Akella, and M. R. Cutkosky. Grasping, manipulation, and control with tactile sensing. In *Proc. IEEE Int. Conf. on Robotics and Automation, ICRA*, Cincinnati, OH, 1990.

[9] T. Inoue and S. Hirai. Elastic model of deformable fingertip for soft-fingered manipulation. *IEEE Trans. in Robotics*, 22:1273–1279, 2006.

[10] T. Inoue and S. Hirai. Quasi-static manipulation using hemispherical soft fingertips by means of minimum d.o.f. two-fingered robotic hand. *J. of the Robotics Society of Japan*, 24:945–953, 2006.

[11] I. Kao and F. Yang. Stiffness and contact mechanics for soft fingers in grasping and manipulation. *the IEEE Trans. of Robotics and Automation*, 20(1):132–135, February 2004.

[12] Y. Li and I. Kao. A review of modeling of soft-contact fingers and stiffness control for dextrous manipulation in robotics. In *Proc. IEEE Int. Conf. on Robotics and Automation, ICRA*, pages 3055–3060, Seoul, Korea, 2001.

[13] J. C. Maxwell. *Philosophical Transactions of the Royal Society London*, 157:49–88, 1867.

[14] D. T. V. Pawluk and R. D. Howe. Dynamic contact of the human fingerpad against a flat surface. *ASME Jour. of Biomechanical Engineering*, vol. 121(6):605–611, 1999.

[15] N. Sakamoto, M. Higashimori, T. Tsuji, and M. Kaneko. An optimum design of robotic hand for handling a visco-elastic object based on maxwell model. In *Proc. IEEE Int. Conf. on Robotics and Automation, ICRA 2007*, pages 1219–1225, Roma, Italy, April 10-14 2007.

[16] K. B. Shimoga and A. A. Goldenberg. Soft robotic fingertips - part I and II: A comparison of construction materials. *Int. Jour. of Robotic Research*, 15(4), 1996.

[17] H. Takagi, M. Takahashi, R. Maeda, Y. Onishi, Y. Iriye, T. Iwasaki, and Y. Hirai. Analysis of time dependent polymer deformation based on a viscoelastic model in thermal imprint process. *Microelectronic Engineering*, 85:902–906, 2008.

[18] P. Tiezzi and I. Kao. Characteristics of contact and limit surface for viscoelastic fingers. In *IEEE Int. Conf. on Robotics and Automation, ICRA 2006*, pages 1365–1370, Orlando, Florida, May 15-19 2006.

[19] P. Tiezzi and I. Kao. Modeling of viscoelastic contacts and evolution of limit surface for robotic contact interface. *IEEE Transaction on Robotics*, 23(2):206–217, April 2007.

[20] P. Tiezzi, I. Kao, and G. Vassura. Effect of layer compliance on frictional behavior of soft robotic fingers. *Advanced Robotics*, 21(14):1653–1670, 2007.

[21] C. D. Tsai and I. Kao. The latency model for viscoelastic contact interface in robotics: Theory and experiments. In *Proc. 2009 IEEE Int. Conf. on Robotics and Automation (ICRA 2009)*, pages 1291–1296, Kobe, Japan, May 2009.

[22] C. D. Tsai, I. Kao, N. Sakamoto, M. Higashimori, and M. Kaneko. Applying viscoelastic contact modeling to grasping task: an experimental case study. In *International Conference on Intelligent Robots and Systems, IROS*, pages 3737–3743, 2008.

[23] N. Xydas and I. Kao. Modeling of contacts and force/moment for anthropomorphic soft fingers. In *Proc. of Int. Conf. on Intelligent Robots and Systems, IROS*, pages 488–493, Victoria, Canada, 1998.

[24] N. Xydas and I. Kao. Modeling of contact mechanics and friction limit surface for soft fingers in robotics, with experimental results. *Int. J. of Robotic Research*, 18(8):941–950, 1999.